*Journal of the Korean Magnetic Resonance Society* **2018**, *22*, 107-114
DOI 10.6564/JKMRS.2018.22.4.107

# $^{207}$Pb nuclear magnetic resonance study in $PbWO_4:Mn^{2+}$ and $PbWO_4:Dy^{3+}$ single crystals

**Tae Ho Yeom***

Department of Laser and Optical Information Engineering, Cheongju University, Cheongju 28503, Republic of Korea

*Received Nov 8, 2018; Revised Dec 11, 2018; Accepted Dec 13, 2018*

**Abstract** In this exploration, the nuclear magnetic resonance of the $^{207}$Pb nucleus in $PbWO_4:Mn^{2+}$ and $PbWO_4:Dy^{3+}$ Single Crystals using FT-NMR spectrometer is investigated. The line width of the resonance line for the $^{207}$Pb nucleus decreases as temperature increases due to motional narrowing. The chemical shift of $^{207}$Pb NMR spectra also increases as temperature decreases for both crystals. The spin-lattice relaxation times $T_1$ of $^{39}$K nucleus were calculated as a function of temperature (180 K~400 K). The $T_1$ of $^{207}$Pb nucleus decreases as temperature increases. The dominant relaxation mechanism at the studied temperature range can be deduced as the Raman process, which is the coupling between lattice vibrations and the nuclear spins. This deduction is substantiated by the fact that the nuclear spin-lattice relaxation rate $1/T_1$ of the $^{207}$Pb nucleus in $PbWO_4:Mn^{2+}$ and $PbWO_4:Dy^{3+}$ single crystal is proportional to $T^2$, or temperature squared. The activation energies for the $^{207}$Pb nucleus in $PbWO_4:Mn^{2+}$ and $PbWO_4:Dy^{3+}$ single crystals are $E_a$ = 49 ± 1 meV and $E_a$ = 47 ± 2 meV, respectively.

**Keywords** $PbWO_4$ single crystal, $Mn^{2+}$ and $Dy^{3+}$ impurities, $^{207}$Pb NMR, spin-lattice relaxation time, activation energy

## Introduction

Lead tungstate ($PbWO_4$) crystals have been intensively studied for the application of high-density scintillator with an inherent luminescence, which has been successfully applied in calorimetric detectors of the Large Hadron Collider (LHC) in CERN[1,2] and have known as heavy scintillation materials in high-energy physics.[3-6] Lead tungstate nano- and macro-crystals have been attracting increasing attention due to their interesting excitonic luminescence, thermos-luminescence, and stimulated Raman scattering behavior.[7] The researches on $PbWO_4$ focused on the light yield increase[8,9] and various doping schemes.[10-12] In the most recent applications in high-energy physics, the crystals are used at a low temperature around 250 K, which considerably changes their radiation damage characteristics,[13] and its mechanism is further explored.[14]

On the other side, $PbWO_4$ crystals also have several laser advantages such as stability, wide infrared transmittance, high thermal conductivity, and high laser damage threshold. $PbWO_4$ is a type of Raman matrix with high qualities and good application prospect in Raman materials.[15] After being doped with rare earth ions, $PbWO_4$ could be a self-stimulated Raman laser material based on its frequency shifting action on the fluorescence of rare earth ions. Several works have been carried out on the Raman laser properties of doped $PbWO_4$ crystals.[16,17]

Characteristics of the $PbWO_4$ emission may be slightly different for various samples. They depend on

* Address correspondence to: **Tae Ho Yeom**, Department of Laser and Optical Information Engineering, Cheongju University, Cheongju 28503, Republic of Korea, Tel: 82-43-229-8555; E-mail: thyeom@cju.ac.kr

growth conditions, quality and impurity composition of the crystals, and mechanical or chemical polishing of the samples.[18] To improve the optical transmittance, decay time, and radiation hardness of $PbWO_4$ scintillating crystals, many researches including doping and annealing treatments have been carried out.[19-21] Several studies on the structural characterization of $PbWO_4$ by X-ray and neutron diffraction techniques have been performed to illustrate the presence of defects in $PbWO_4$ crystals.[22,23] The majority of dopants in $PbWO_4$ are considered to replace the $Pb^{2+}$ ions and compensate the $Pb^{2+}$ deficiency. Kobayashi et al. reported that the scintillating properties could be significantly improved by doping trivalent ions.[24] They considered that these ions could compensate the $Pb^{2+}$ deficiency, thus reducing the defects.

$PbWO_4$ crystal doped with $Dy^{3+}$ exhibit improved transmittance in the short wavelength region. In $Dy:PbWO_4$, the $WO_4^{2-}$ group can absorb excitation energy and transfer part of the energy to the $Dy^{3+}$ ions, followed by the strong luminescence of $Dy^{3+}$.[25] $Mn^{2+}$ is also frequently used as a dopant to improve phosphors. The conjectured $Pb^{2+}$ deficiency due to evaporation can occur not only during crystal growth but also during annealing.[26] Nuclear magnetic resonance (NMR) method is very suitable for investigating microscopic information of materials. The spin-lattice relaxation time of the nuclei in host single crystals reflects the dynamics of the sample crystals, for instance the spin-phonon interaction, and shows how easily the excited state energy of the nuclear spin system can be transferred into the lattice. The NMR studies of $PbWO_4$ single crystals doped with $Mn^{2+}$ and $Dy^{3+}$ are not reported so far. In this paper, the $^{207}Pb$ NMR spectra in $PbWO_4:Mn^{2+}$ and $PbWO_4:Dy^{3+}$ single crystals at the temperature range 180 K~410 K are obtained. The chemical shift, linewidth, and intensity of the $^{207}Pb$ NMR spectra are also discussed. The spin-lattice relaxation time of $^{207}Pb$ nuclei in both crystals were measured using Fourier transform (FT) NMR spectrometer in order to obtain specific information regarding the dynamics of $PbWO_4$ crystals doped with paramagnetic impurities. The activation energy of $^{207}Pb$ nuclei are calculated. This investigation that studies the NMR of the $PbWO_4$ single crystals doped with $Mn^{2+}$ and $Dy^{3+}$ impurity ions have not been previously reported.

## Crystal Structure and Experimental Aspects

The scheelite $PbWO_4$ crystal structure is tetragonal with space group $I41/a$. The lattice constants of the unit-cell are $a = b = 0.5456$ nm and $c = 1.2020$ nm.[27] The unit cell consists of four molecules. The W and Pb sites in $PbWO_4$ single crystal have S4 point symmetry. The $Pb^{2+}$ and $W^{6+}$ ions are surrounded by eight oxygen atoms and four oxygen atoms, respectively. The W ions in $PbWO_4$ crystals are located in two types of oxygen tetrahedra, which are slightly rotated with respect to each other.[28] The melting point of $PbWO_4$ single crystal is 1123 $^oC$.

The NMR spectra of $^{207}Pb$ in $PbWO_4:Mn^{2+}$ and $PbWO_4:Dy^{3+}$ single crystals were measured by the Bruker Solid-state NMR spectrometer (DSX 400 MHz) at the Korea Basic Science Institute. The static magnetic field was 9.4 T and the Lamor frequency (central radio frequency) was set to $\omega_o/2\pi = 83.538$ MHz for the $^{207}Pb$ nucleus. The spin-lattice relaxation time $T_1$ was measured using the saturation recovery pulse sequence ($\pi/2$-$\tau$-$\pi$) for the $^{207}Pb$ nucleus. The delay times for the measurement of $T_1$ and for Fourier transform NMR resonance line of $^{207}Pb$ nucleus are 1 s and 10 s, respectively. The temperature-dependent $^{207}Pb$ nuclei resonance lines in the crystals were obtained within the temperature range of 180-410 K. The sample temperatures were maintained constant by adjusting the nitrogen gas flow and heater current. The saturation recovery traces of the $^{207}Pb$ nucleus in a $PbWO_4:Dy^{3+}$ single crystal were obtained as a function of delay time and the results are shown in Figure 1.

## Analysis and Discussion

The temperature dependence of the $^{207}Pb$ NMR spectrum in $PbWO_4:Mn^{2+}$ and $PbWO_4:Dy^{3+}$ single crystals was measured at 13 different temperatures in

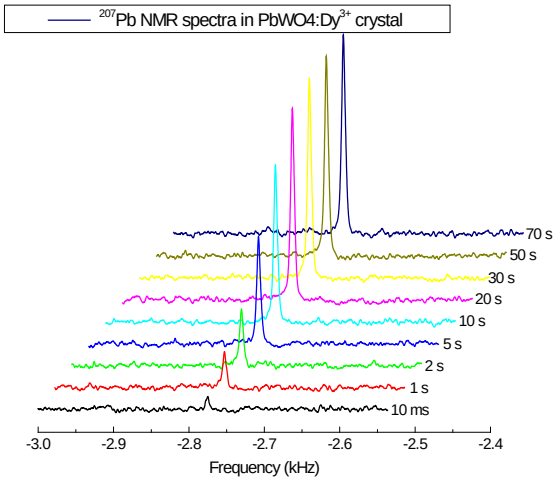


**Figure 1.** Saturation recovery traces of the $^{207}$Pb nucleus in a $PbWO_4$:$Dy^{3+}$ single crystal as a function of delay time at 300 K**.**

the range 180 K~410 K. The typical FT NMR spectra for the $^{207}$Pb nuclei in both single crystals at several temperatures are shown in Figure 2. This spectrum is obtained by a Fourier transform of the free induction decay for $^{207}$Pb NMR. Only one resonance line is measured as expected from the nuclear spin I = 1/2 for $^{207}$Pb. This single resonance line shows that there is only one chemically and magnetically equivalent $^{207}$Pb site in the $PbWO_4$ crystal. All $^{207}$Pb resonance frequencies of $PbWO_4$:$Mn^{2+}$ and $PbWO_4$:$Dy^{3+}$ single crystals in Figure 2 (a) and (b) are shifted from the zero point of the frequency (= 83.538 MHz) of the bare $^{207}$Pb NMR. In general, the resonance frequency of nucleus in the crystal is different for a nucleus embedded in crystal from that of a 'bare' nucleus. These frequency shifts are originated from the chemical shift.[29] The spectra in Figure 2(a) and in Figure 2(b) at 300 K are shifted by -2.868 kHz for the $PbWO_4$:$Mn^{2+}$ crystal and by -2.777 kHz for the $PbWO_4$:$Dy^{3+}$ crystal from the operating frequency $\omega_o/2\pi$ = 83.538 MHz, respectively, due to the chemical shift.

The temperature dependence of resonance frequency for the $^{207}$Pb nuclei in $PbWO_4$:$Mn^{2+}$ and $PbWO_4$:$Dy^{3+}$ single crystals is shown in Figure 3. The resonance frequency of the $^{207}$Pb nuclei in both crystals is closer

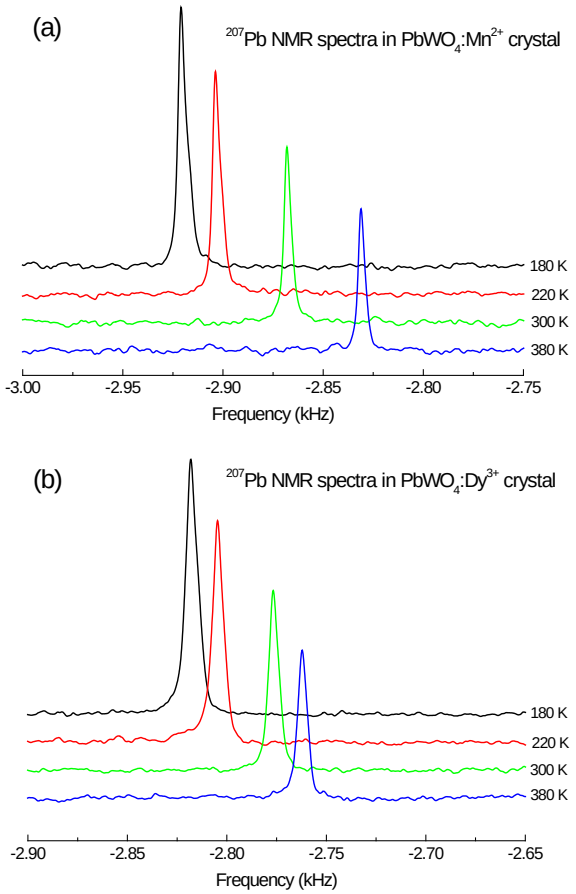


**Figure 2.** Typical NMR spectra of the $^{207}$Pb nucleus (a) in $PbWO_4$:$Mn^{2+}$ (b) in $PbwO_4$:$Dy^{3+}$ single crystals at several temperatures operating at $\omega_o/2\pi$ = 83.538 MHz.

to the zero point of the frequency when temperature increases. The solid lines in Figure 3 are the linear fit of the resonance frequencies of the $^{207}$Pb nuclei with increasing temperature for both crystals. The chemical shift of the $^{207}$Pb nucleus in the $PbWO_4$:$Mn^{2+}$ crystal is stronger than that in the $PbWO_4$:$Dy^{3+}$ crystal at all temperatures within the range investigated. The chemical shifts of $^{207}$Pb NMR lines in $PbWO_4$:$Mn^{2+}$ and $PbWO_4$:$Dy^{3+}$ single crystals linearly decrease when temperature increases.

The peak to peak intensities of the $^{207}$Pb NMR spectra in $PbWO_4$:$Mn^{2+}$ and $PbWO_4$:$Dy^{3+}$ single crystals decreased with increasing temperature for all temperature range as shown in Figure 4. The

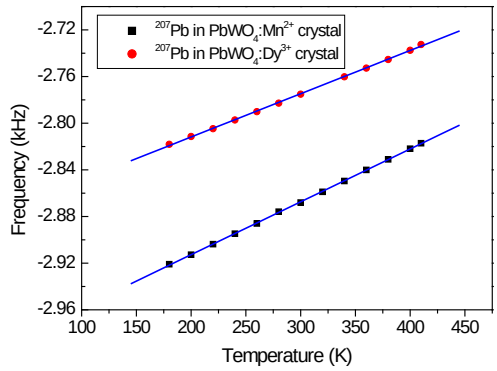


**Figure 3.** Resonance frequency of the $^{207}Pb$ nuclei in $PbWO_4:Mn^{2+}$ and $PbWO_4:Dy^{3+}$ single crystals as a function of temperature. The zero point is the Larmor frequency 83.538 MHz.

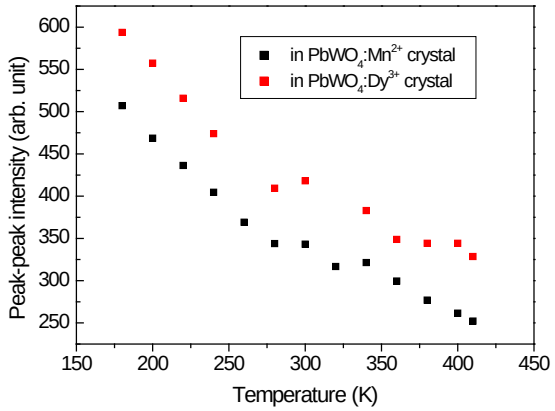


**Figure 4.** Peak to peak intensity of the $^{207}Pb$ NMR line in $PbWO_4:Mn^{2+}$ and $PbWO_4:Dy^{3+}$ single crystals as a function of temperature.

linewidths of the $^{207}Pb$ nuclei in $PbWO_4:Mn^{2+}$ and $PbWO_4:Dy^{3+}$ single crystals are $(\Delta\nu)_{FWHM}$ = 4.2 Hz and $(\Delta\nu)_{FWHM}$ = 6.0 Hz at 300 K (see Figure 5). The linewidth at FWHM (full width at half maximum) of the resonance line for the $^{207}Pb$ NMR decreases with increasing temperature due to motional narrowing. The linewidth of the $^{207}Pb$ nucleus in $PbWO_4:Mn^{2+}$ is smaller than that in $PbWO_4:Dy^{3+}$ single crystals. The differences of chemical shift and FWHM for $^{207}Pb$ NMR spectra in two different $PbWO_4:Mn^{2+}$ and $PbWO_4:Dy^{3+}$ crystals may originate from the crystal growing conditions rather than different impurities

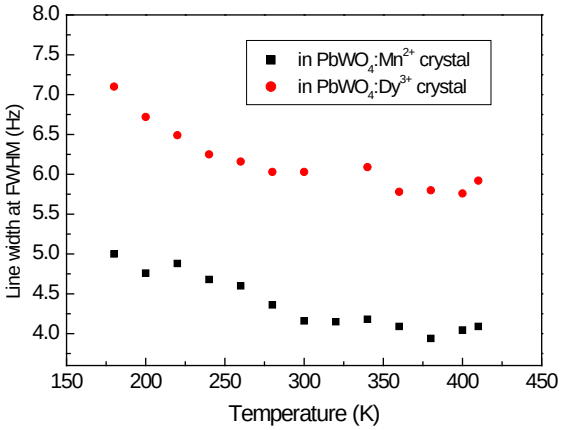


**Figure 5.** Linewidth (FWHM) of the $^{207}Pb$ NMR line in $PbWO_4:Mn^{2+}$ and $PbWO_4:Dy^{3+}$ single crystals as a function of temperature.

because both impurity concentrations in the crystals are not high.

The saturation recovery traces of the nuclear magnetization were measured at the temperature range 180~410 K for the $^{207}Pb$ nucleus. The obtained magnetization recoveries $[M(\infty) - M(t)]/2M(\infty)$ for $^{207}Pb$ (I = 1/2, natural abundance 22.6%) nucleus were found to fit a single exponential function with the following equation:[30-32]

$$[M(\infty) - M(t)]/2M(\infty) = \exp(-t/T_1) \qquad (1)$$

where $M(\infty)$ denotes the nuclear magnetization at thermal equilibrium, $M(t)$ the magnetization of the transition for $^{207}Pb$ nucleus at time $t$, and $T_1$ the spin-lattice relaxation time. The magnetization recovery traces at several temperature are shown in Figure 6.

The coupling between the lattice vibrations and the spins can be generally be written using a spin-lattice Hamiltonian.[29] Lattice operator can be expanded as a function of the stress. At the temperature far below the melting point of the single crystal, we can reasonably presume that the thermal stress is small and only the first few terms of lattice operator are important. The first order term shows the direct process, which is the absorption or emission of a single phonon. However, this term is negligibly small. The physical reason for the inefficiency of the direct process is that only phonons in the neighborhood of the frequency

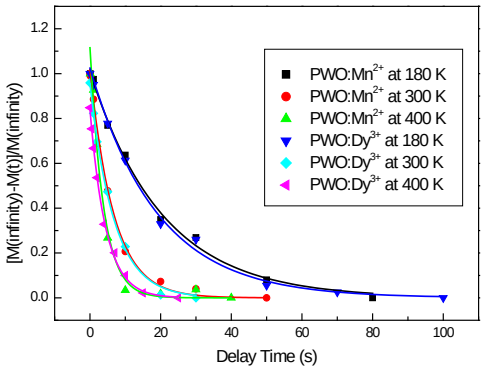


**Figure 6.** Magnetization recovery traces for $^{207}$Pb nuclei in $PbWO_4:Mn^{2+}$ and $PbWO_4:Dy^{3+}$ crystals. The curves are fitted with eq. (1).

contribute to the relaxation and that the corresponding spectral density of thermal energy is very small. The succeeding second order term is the two-phonon processes (Raman process). The absorption of one phonon and the emission of the other is overwhelmingly more important than the emission or absorption of two phonons. The Raman Process shows the relaxation rate, $1/T_1$, is proportional to the square of the temperature in the high temperature limit.[29,33,34] Another two-phonon process is the Orbach process. However, this process shows an exponential relationship between the relaxation rate and temperature.[29]

From the magnetization of the $^{207}$Pb nuclei in $PbWO_4:Mn^{2+}$ and $PbWO_4:Dy^{3+}$ single crystals, spin-relaxation times were calculated with eq. (1) in the temperature range 180 K ~ 410 K. The temperature dependence of the nuclear spin-lattice relaxation rate $1/T_1$ for $^{207}$Pb nuclei was obtained and shown in Figure 7. The relaxation time of the $^{207}$Pb nuclei shows no abrupt changes in the experimental temperature range, which means that no physical abrupt changes occur. The $1/T_1$ values of the $^{207}$Pb nuclei in both crystals were found to increase when temperature increases. This is rational because the lattice vibration is more effective when the crystal temperature is increased, the relaxation time becomes shorter with increasing temperature.

The relaxation mechanism for the $^{207}$Pb NMR in $PbWO_4:Mn^{2+}$ and $PbWO_4:Dy^{3+}$ single crystals can be explained in terms of lattice vibration and nuclear spin. The relaxation rates of $^{207}$Pb nuclei in both crystals are proportional to the square of temperature in the investigated temperature range as indicated with solid lines in Figure 7. Therefore, the temperature dependence of the $^{207}$Pb relaxation rate in PbWO4 crystals is in accordance with Raman processes. Though our measurement was made with a single crystal samples doped with $Mn^{2+}$ and $Dy^{3+}$ impurities, the relaxation process represents a more reliable feature of the intrinsic behavior of the $PbWO_4:Mn^{2+}$ and $PbWO_4:Dy^{3+}$ single crystals. Namely, the Raman process is more effective than the paramagnetic impurity effects in our experiment.

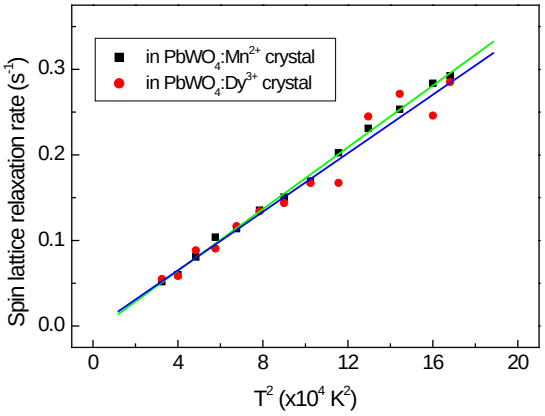


**Figure 7.** Temperature dependence of the spin-lattice relaxation rate $1/T_1$ for the $^{207}$Pb in $PbWO_4:Mn^{2+}$ and $PbWO_4:Dy^{3+}$ single crystals. The solid line is fits obtained by assuming Raman processes.

The activation energy of the $^{207}$Pb nuclei in $PbWO_4:Mn^{2+}$ and $PbWO_4:Dy^{3+}$ single crystals was obtained from the equation $T_1 = A_o exp(E_a/k_B T)$,[29,35] where $A_o$ and $E_a$ denote the pre-exponential factor and the activation energy, respectively. The constants $k_B$ and $T$ denote the Boltzmann constant and the temperature, respectively. A linear plot of the natural logarithm of relaxation time $T_1$ as a function of inverse temperature is shown in Figure 8. The gradient of the linear fits is related to the activation energy of the $^{207}$Pb nuclei. The activation energies of the $^{207}$Pb nuclei

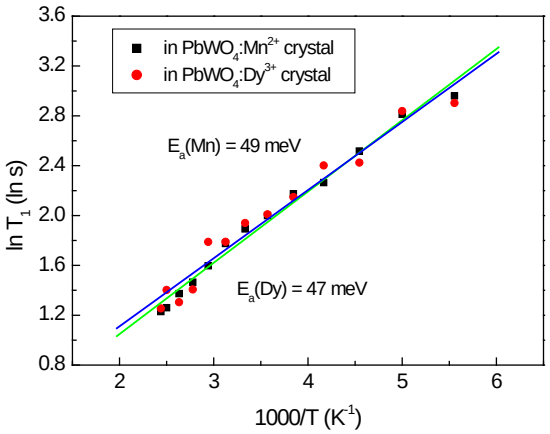


**Figure 8.** The spin-lattice relaxation time of the $^{207}Pb$ nucleus vs. the reciprocal temperature in the experimental temperature region. The slope of the solid line represents the activation energy**.**

obtained from the slope of the graph in Figure 8 are $E_a$ = 49 ± 1 meV for $PbWO_4:Mn^{2+}$ crystal and $E_a$ = 47 ± 2 meV for $PbWO_4:Dy^{3+}$ single crystal, respectively. These activation energies are required to activate the nucleus and to allow the participation in the spin-lattice relaxation process of the of $^{207}Pb$ nucleus in $PbWO_4:Mn^{2+}$ and $PbWO_4:Dy^{3+}$ single crystals. The values of activation energies of $^{207}Pb$ nuclei in both crystals are the same within the experimental accuracy. This may show that paramagnetic impurity effects on relaxation is almost negligible because $T_1$ of $^{207}Pb$ nuclei in both crystals doped with different paramagnetic ions ($Mn^{2+}$: $3d^5$ and $Dy^{3+}$: $4f^9$) has no difference. Only the intrinsic component is effective for the relaxation of $^{207}Pb$ nuclei instead of paramagnetic impurities.

## Summary

The NMR of the $^{207}Pb$ nucleus in $PbWO_4:Mn^{2+}$ and $PbWO_4:Dy^{3+}$ single crystals have been investigated by employing the FT-NMR spectrometer in the temperature range of 180 K~410 K. Only one $^{207}Pb$ resonance line was obtained in both crystals. This indicates that there is only one chemically and magnetically equivalent $^{207}Pb$ site in the host crystals. The chemical shifts of $^{207}Pb$ resonance lines in $PbWO_4:Mn^{2+}$ and $PbWO_4:Dy^{3+}$ single crystals decrease linearly when temperature increases. The chemical shift of the $^{207}Pb$ nucleus in $PbWO_4$ crystal doped with $Mn^{2+}$ ion is stronger than that in $PbWO_4$ crystal doped with $Dy^{3+}$ ion at all temperature range. The line width and peak to peak intensity of the $^{207}Pb$ nuclei in both crystals decrease with increasing temperature.

The relaxation mechanism of the $^{207}Pb$ nuclei was investigated by describing the spin-lattice relaxation time, $T_1$, of the $^{207}Pb$ as a function of temperature in $PbWO_4:Mn^{2+}$ and $PbWO_4:Dy^{3+}$ single crystals. The spin-lattice relaxation time $T_1$ values of the $^{207}Pb$ nuclei in PbWO4 single crystals continuously decreased with increasing temperature. This shows that no phase transitions occurs within the experimental temperature range. The Raman process is the dominant relaxation mechanism for $^{207}Pb$ NMR in the temperature range. This is because the spin-lattice relaxation rate $1/T_1$ of the $^{207}Pb$ nuclei in in $PbWO_4:Mn^{2+}$ and $PbWO_4:Dy^{3+}$ single crystals is proportional to the square of temperature ($T^2$). The lattice vibrations in the host crystals are coupled to the nuclear spin via Raman spin-phonon coupling.

The activation energies obtained for the $^{207}Pb$ nuclei in $PbWO_4:Mn^{2+}$ and $PbWO_4:Dy^{3+}$ single crystals are $E_a$ = 49 ± 1 meV and $E_a$ = 47 ± 2 meV, respectively. These activation energy of $^{207}Pb$ nuclei for $PbWO_4$ doped with $Mn^{2+}$ impurity is the same as that for $PbWO_4$ doped with $Dy^{3+}$ impurity within the experimental errors. Therefore, the paramagnetic impurity effect on the relaxation of $^{207}Pb$ in $PbWO_4$ crystals is almost negligible and the Raman process is dominant in the experimental temperature range investigated.

## References

1. Compact Muon Solenoid Technical Proposal, CERN/LHCC 94-38, LHCC, P1 (1994)
2. P. Lecoq, I. Dafinei, E. Auffray, M. Schneegans, M.V. Korzhik, O.V. Missevitch, V.B. Pavlenko, A.A.

Fedorov, A.N. Annenkov, and V.L. Kostylev, *Nucl. Instrum. Methods Phys. Res. A* **365**, 291 (1995)
3. P. Lecoq, *Nucl. Instrum. Methods Phys. Res. A* **537**, 15 (2005)
4. M. Kobayashi, M. Ishii, Y. Usuki, and H. Yahagi, *Nucl. Instrum. Methods Phys. Res. A* **333**, 429 (1993)
5. M. Nikl, *Phys. Status Solidi A* **178**, 595 (2000)
6. A. N. Caruso, *J. Phys.: Condens. Matter* **22**, 443201 (2010)
7. M. Kobayashi, M. Ishii, and Y. Usuki, *Nucl. Instrum. Methods Phys. Res. A* **406**, 442 (1998)
8. M. Nikl, P. Bohacek, A. Vedda, M. Martini, G.P. Pazzi, P. Fabeni, and M. Kobayashi, *Phys. Status Solidi A* **182**, R3 (2000)
9. A.A. Annenkov, A.E. Borisevich, A. Hofstaetter, M.V. Korzhik, P. Lecoq, V.D. Ligun, O.V. Misevitch, R. Novotny, and J.P. Peigneux, *Nucl. Instrum. Methods. Phys. Res. A* **450**, 71 (2000)
10. M. Kobayashi, Y. Usuki, M. Ishii, M. Itoh, and M. Nikl, *Nucl. Instrum. Methods. Phys. Res. A* **540**, 381 (2005)
11. G.-H. Ren, X.-F. Chen, R.-H. Mao, and D.-Z. Shen, *Acta Phys. Sin.* **59**, 4812 (2010)
12. C. Ye, J. Liao, P. Shao, and J. Xie, *Nucl. Instrum. Methods. Phys. Res. A* **566**, 757 (2006)
13. R.W. Novotny, W.M. D¨ oring, V. Dormenev, A. Hofstaetter, M. Korzhik, T. Kuske, S. Lugert, and O. Missevitch, *IEEE Nucl. Sci. Symp. Conf. Rec.*, Art 5402124, 2036 (2009)
14. S. Burachas, M. Ippolitov, V. Manko, S. Nikulin, A. Vasiliev, A. Apanasenko, A. Vasiliev, A. Uzunian, and G. Tamulaitis, *Radiat. Meas.* **45**, 83 (2010)
15. A. A. Kaminskii, C. L. McCray, H. R. Lee, S. W. Lee, D. A. Temple, T. H. Chyba, W. D. Marsh, J. C. Barnes, A. N. Annanenkov, V. D. Legun, H. J. Eichler, G. M. A. Gad, and K. Ueda, *Opt. Commun.* **183**, 277 (2000)
16. I. S. Mirov, V. V. Fedorov, I. S. Moskalev, D. V. Martyshkin, S. Y. Beloglovski, S. F. Burachas, Y. A. Saveliev, and A. M. Tseitline, *Opt. Mater.* **31**, 94 (2008)
17. W.B. Chen, Y. Inagawa, T. Omatsu, M. Tateda, N. Takeuchi, and Y. Usuki, *Opt. Commun.* **194**, 401 (2001)
18. S. Zazubovich, and M. Nikl, *Phys. State Solid (b)* **247**, 385 (2010)
19. R.Y. Zhu, D.A. Ma, H.B. Newman, C.L.Woody, J.A. Kierstead, S.P. Stoll, and P.W. Levy, *Nucl. Instr. Meth. A* **376**, 319 (1996)
20. A. Annenkov, E. Auffray, M.V. Korzhik, P. Lecoq, and J.-P. Peigneux, *Phys. Status Solidi A* **170**, 47 (1998)
21. B. Han, X. Feng, G. Hu, Y. Zhang, and Z. Yin, *J. Appl. Phys.* **86**, 3571 (1999)
22. J. M. Moreau, Ph. Galez, J.P. Peigneux, and M.V. Korzhik, *J. Alloys Comp.* **46**, 238 (1996)
23. J. M. Moreau, R. E. Gladyshevskii, Ph. Galez, J.P. Peigneux, and M.V. Korzhik, *J. Alloys Comp.* **284**, 104 (1999)
24. M. Kobayashi, Y. Usuki, M. Ishii, N. Senguttuvan, K. Tanji, M. Chiba, K. Hara, H. Takano, M. Nikl, P. Bohacek, S. Baccaro, A. Cecilia, and M. Diemoz, *Nucl. Instr. Meth. A* **434**, 412 (1999)
25. Y. Huang, W. Zhu, X. Feng, Z. Liu, Z. Man, and Z. Yin, *Opt. Mater.* **23**, 443 (2003)
26. M. Kobayashi, Y. Ushki, M. Ishii, N. Senguttuvan, K. Tanji, M. Chiba, K. Hara, H. Takano, M. Nikl, P. Bohacek, S. Baccaro, A. Cecilia, M. Diemoz, A. Vedda, and M. Martini, *Nucl. Instrum. Methods Phys. Res. A* **465**, 428 (2001)
27. A. A. Kaminskii, C.L. McCray, H. R. Lee, S. W. Lee, D. A. Temple, T. H. Chyba, W. D. Marsh, J. C. Barnes, A. N. Annanenkov, V. D. Legun, H. J. Eichler, G. M. A. Gad, and K. Ueda, *Opt. Commun.* **183**, 277 (2000)
28. L. Z. Leciejewitz, *Z. Kristallogr.* **121**, 158 (1965)
29. A. Abragam, "The Principles of Nuclear Magnetism" Chaps. VI, VI1, and IX, Oxford Univ. Press, Oxford, 1961
30. W. W. Simmons, W. J. O'Sullivan, and W. A. Robinson, *Phys. Rev.* **127**, 1168 (1962)
31. W. E. Blumberg, *Phys. Rev.* **119**, 79 (1960)
32. A. R. Lim and K. Y. Lim, *Solid State Sci.* **31**, 70 (2014)
33. R. L. Mieher, *Phys. Rev.* **125**, 1537 (1962)

34. J. Van Kranendonk, *Physica* **20**, 781 (1954)
35. A. R. Lim, *AIP Adv.* **6**, 35307 (2016)